Change of opinion allows coexistence of competing memes in the same social network

Ricardo Riol and Simone Santini

Abstract—We present a model of double viral spreading on a multi-network suitable for modeling the diffusion of competitive memes. The main characteristics of the model is that it allows the possibility of changing from one opinion to another without having to go through an agnostic (susceptible) phase.
We analyze the survival of two conflicting memes in the limit of $t \to \infty$ as a function of the effective viralities $\tau = \beta_p/\delta_p$ and $\theta = \beta_q/\delta_q$, and using as parameters the cross-meme viralities $\alpha_p = \beta(p \to q)\beta_p$ and $\alpha_q = \beta(p \to p)\beta_q$. The parameter space is divided into four survival regions, depending on which meme survives (none, one of the two, both). We derive exact equations for the boundaries between the regions in the case of regular graphs, and qualitative equations for the general case.
One relevant finding is that, contrary to the viral spread model in [27], the crossover allows the co-existence of two memes in the same network. We present simulations to validate the theoretical results.

Index Terms—

1 Introduction

Multiple viral spreading on one network, or on multiple networks defined on the same nodes, has attracted substantial attention thanks to the rich dynamics it generates [1], [10], [15], [37]. The idea and the models of viral spreading originated in the study of the diffusion of pathogens [25], [30], and from there they spreaded (pun intended) to the analysis of many other problems that exhibit a similar dynamics, from product diffusion [2], to worm propagation in computer networks [13].

One area in which viral models have received much attention is that of information diffusion and opinion formation in social networks. Work in this area can be roughly divided in two groups [6].

On the one hand, there are models of opinion formation [4], [29]. Opinion is a stochastic process with a continuous range. In general, for individual i, the opinion at time t is $o_i(t) \in [-1, 1]$, varying continuosly between two "extremist" positions with $o_i(t) = 0$ representing either a centrist or an indifferent position. The main techniques in this area are game-theoretic [19], studying in particular the existence of Nash equilibria [21], or kinetic exchange models [16], [33], which build on equilibria of gas dynamic models [8]. Different approaches consider $o_i \in \{0, 1\}$ and apply Ising [], voting [] or Sznadj [31] models. Variations may be introduced, such as the presence of a recommender system [29] or the presence of information sources of fixed opinion with confirmation bias [18].

On the other hand, we have the study of meme spreading [20], [32]. In this case, meme acceptance is assumed to be a binary stochastic process: at any time, each individual either believes a meme or doesn't. Several techniques have been used in this area, from game-theoretic models [14], to experimental studies [9], and viral models [28]. One interesting variation of this model is the consideration of *two* incompatible memes (viz., it is assumed that a reasonable person cannot believe both memes to be true at the same time, thus explicitly excluding the possibility of *doublethink* [24]). In this case, it is often assumed that the two may spread on different networks defined on the same individuals [20], [36]. This is the problem that we shall consider in this paper. Here too there are variants defined in the model, from the effects of limited attention [38] to the effects of clustering [40].

Accurately modeling multiple viral diffusion is a complex problem due to the different manners in which the spreading elements may interact: they may reinforce each other [22], weaken each other [12], or exclude each other [23]; the relation between them may be symmetrical or asymmetrical [1], [39]. The most common simplifying assumption is that of the SI_2I_2S model [27]: two viruses act independently on susceptible (healthy) individuals, and they are synchronically exclusive (a person infected with virus 1 cannot be at the same time infected by virus 2) as well as diachronically (a person with virus 1 must become susceptible again before they may be infected by virus 2). Synchronic exclusivity can be applied to the case of meme diffusion, being a consequence of the assumption that there is no doublethink. Diachronical exclusivity, on the other hand, has no evident modeling counterpart for meme diffusion, since one person can indeed change their mind from believing one meme to believing another without necessarily going through a neutral or agnostic state. In this pape we shall study the consequences of dropping the diachronical exclusivity hypothesis.

• *Escuela Politécnica Superior, Universidad Autónoma de Madrid, 28043 Madrid, Spain*
E-mail: simone.santini@uam.es,ricardo.riol@estudiante.uam.es

Manuscript received XXX; revised XXX. Simone Santini was supported in part by the Spanish Ministerio de Educación y Ciencia under the grant N. TIN2016-80630-P, Recomendación en medios sociales: contexto, diversidad y sesgo algorítmico.

Multiple viral diffusion has been studied using several techniques, among which two classes stand out. *Bond percolation* [23] assumes that an infected person has only one chance to infect its neighbors and that once infected it never becomes susceptible again. In this way, one can model the problem as a random removal of graph edges, and the spread of the virus can be modeled as percolation in the resulting graph. The original model [23] assumed that the viruses spread one at the time on the same network, but the model has been extended to simultaneous spread [15] as well as to two-layer networks [10].

A second type of solutions considers viral spreading as a *Markov process* in which the state is given by the epidemiological status of each individual. The complete model is intractable: for a single virus and two possible stati (S, I), on a network with N individuals, the model has 2^N states [11], [34]. In order to make the model tractable, approximations such as mean field are used [27], [28].

One of the most significant and general results for a single virus spread is the existence of a spreading threshold, which depends on the epidemiological constants as well as on the structure of the network. If β is the infection rate of the virus, δ is the recovery rate, and $\tau = \beta/\delta$ is the effective infection rate, then the virus spreads if $\tau > 1/\lambda_1$, where λ_1 is the largest eigenvalue of the network [28]. This result shows that vulnerability to viral spread is a characteristic of the network: λ_1 is never smaller than the mean degree of the network, limiting the resilience of networks with many links. Also, for example, Erdös-Renyi graphs [5] have a larger spectral radius than scale-free graphs [3] with the same average connectivity, and are therefore, *cœteris paribus*, more vulnerable to viral spread.

When two viruses are involved, the main results are related to the possible coexistence of the two vis-à-vis the dominance of one of them. Wang *at al.* [35] proved that competitive, exclusive viruses cannot coexist in scale-free networks, and Prakash *et al.* [26] extended the result to arbitrary networks. Viruses can spread using different infection modalities, a situation that is modeled with the use of multi-networks: independent sets of edges on the same set of nodes (compare, for example, airborne vs. sexually transmitted viruses: the network on which the first virus spreads will be more dense than that on which the second does). For two viruses, the model is a multi-network $G = (V, E_1, E_2)$ with $E_1, E_2 \subseteq V \times V$. Darabi and Scoglio [27] analyze this model and determine the threshold under which both viruses die out as well as the thresholds for survival and dominance of each virus. Their results are that the virus may coexist if $E_1 \neq E_2$, but that coexistence on a single network is impossible.

As we have already mentioned, all this work uses the strict competitive-exclusive virus model SI_1I_2S: each node can be infected by only one virus at a time, and only susceptible individuals can be infected. This entails that a person infected with virus 1 can't immediately become infected with virus 2: they must first recover from the first virus in order to become susceptible to the second, that is, the two viruses are assumed to be diachronically exclusive.

If we apply viral spreading to the diffusion of memes and the opinions about them, this model is no longer appropriate. If the two "viruses" represent two incompatible memes and no doublethink is assumed, synchronic exclusivity still applies. On the other hand, in the case of memes, it is possible to change opinion instantaneously: persons that at a given moment hold meme 1 to be true may suddenly change their mind and hold meme 2 to be true without having to go through an "agnostic" (viz., susceptible) state: diachronic exclusivity does not apply. This is the model that we analyze in this paper, a model that is an extension of the *fact-checking* one proposed in [32]. We show that the extinction threshold is not affected by the change, while the behavior of the infection above the threshold shows an important change: the two memes can coexist on a single network.

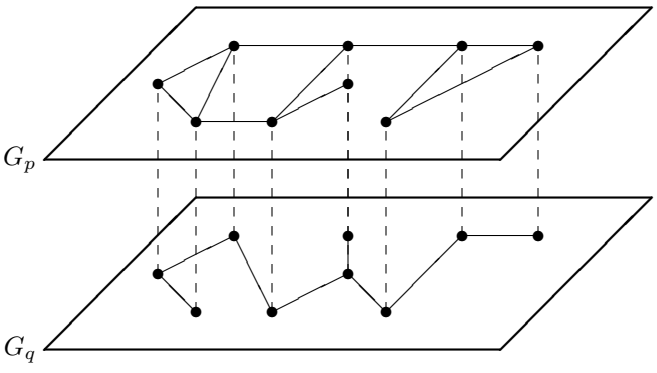

Fig. 1. Schematic view of the multi-network model. The model is composed of a set of nodes (V) and two independent sets of edges between them (E_p and E_q). The model can be projected on either set of edges obtaining the propagation graphs $G_p = (V, E_p)$ and $G_q = (V, E_q)$.

2 THE MODEL

We use here a model based on competitive, exclusive memes spreading over a two-layer network, derived from that in [27], and originally proposed in [36].

Consider a population of N individuals, and two memes that propagate along different routes (e.g., one meme may propagate through broadcast radio and the other through word of mouth). Our model is a multi-network $G = (V, E_p, E_q)$, where $V = \{1, \ldots, N\}$ is the set of individuals, $E_p \subseteq V \times V$ is the set of links along which the first meme propagates (henceforth: meme 1 or meme p), and $E_q \subseteq V \times V$ is the set of links along which the second meme propagates (meme 2 or meme q), see Figure 1. We shall on occasion use the "projections" of the network on its two component graphs $G_p = (V, E_p)$ and $G_q = (V, E_q)$. Define the adjacency matrices $\mathbf{A} = \{a_{ij}\}$ and $\mathbf{B} = \{b_{ij}\}$ with elements

$$a_{ij} = \begin{cases} 1 & (i,j) \in E_p \\ 0 & \text{otherwise} \end{cases}$$
$$b_{ij} = \begin{cases} 1 & (i,j) \in E_q \\ 0 & \text{otherwise} \end{cases} \quad (1)$$

We assume that the graphs are undirected ($\mathbf{A} = \mathbf{A}'$ and $\mathbf{B} = \mathbf{B}'$). Let $d_i^A = \sum_j a_{ij}$ be the $\mathbf{A}$-degree of node i, set $\mathbf{d}^A = [d_1^A, \ldots, d_N^A]'$, $\mathbf{D}_A = \text{diag}(d_1^A, \ldots, d_N^A)$. Let $\lambda_A = \lambda_1(\mathbf{A})$ be the largest eigenvalue of $\mathbf{A}$, and $\mathfrak{a} = [\mathfrak{a}_1, \ldots, \mathfrak{a}_N]'$ be the corresponding unitary eigenvector. The

corresponding values for $\mathbf{B}$, d_i^B, $\mathbf{d}^B$, $\mathbf{D}^B$, λ_B, and $\mathfrak{b}$ are defined analogously.

The individuals are modeled using a modified SI_1I_2S model: each node of the network is, at any time, in one of three possible states (S, I_p, I_q) that, in the meme scenario, are interpreted as follows:

- S susceptible. The individual is agnostic, with no opinion regarding the truth of either meme. This can be due to the individual not having been in contact with the memes, to the individual not having made up their mind as to the truth of either meme, or to the individual having grown skeptical or indifferent about the truth of a meme that they previously held true.
- I_p p-infected. The individual believes that the meme p is true (and, consequently, because of synchronic exclusivity, that meme q is false).
- I_q q-infected. The symmetric relation: the individual believes that q is true and p is false.

No individual can believe p and q simultaneously. In our model, belief is active, and includes proselytism, so individuals that (actively) believe a meme will try to convince their neighbors. Individuals that privately believe the meme but do not communicate it and do not proselitize will be in state S. Similarly, individuals that keep passively believeing the meme but do not propagate their belief anymore will be considered to have returned to state S. This complication is inherent to our interpretation and does not appear in the virus scenario since a person affected by a virus cannot voluntarily control their potential to infect. The basic process is similar to that used in [27] for the case of viruses and [32] for memes. The infection and curing processes for the two memes are characterized by the parameters (β_p, δ_p) and (β_q, δ_q) respectively. The process is represented schematically as follows:

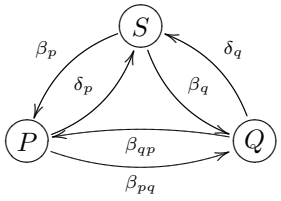

(2)

Let an individual have, at time t, $N_p(t)$ neighbors that believe p and $N_q(t)$ that believe q. Then the individual can change state according to the following processes:

From state S

- a p-believing process: Poisson process with rate $\beta_p N_p(t)$ leading to state I_p;
- a q-believing process: Poisson process with rate $\beta_q N_q(t)$ leading to state I_q.

From state I_p

- a disbelieving process, with rate δ_p, leading to state S;
- a change-to-q process with rate $\beta_{pq} N_q(t)$ leading to state I_q.

From state I_q

- a disbelieving process, with rate δ_q, leading to state S;
- a change-to-p process with rate $\beta_{qp} N_p(t)$ leading to state I_p.

We shall consider that β_{qp} is proportional to β_p and that β_{pq} is proportional to β_q: $\beta_{qp} = \alpha_q \beta_p$, and $\beta_{pq} = \alpha_p \beta_q$. The rationale here is that if a meme is "strong", in the sense that it may convince people without any specific belief, it is also "strong" in the sense that it can convince people to change their mind. The parameters α_p and α_q will be assumed to be constant.

The semantics of the model entails two conditions. The first is

$$\begin{aligned} \beta_{qp} &> \beta_p \delta_q \\ \beta_{pq} &> \beta_q \delta_p. \end{aligned} \tag{3}$$

This means that convincing is effective, that is, it is easier to change somebody's mind than wait for that person to become agnostic and then trying to convince them; we call this a *limited resilience* clause. The second is

$$\begin{aligned} \beta_{qp} &< \beta_p \\ \beta_{pq} &< \beta_q; \end{aligned} \tag{4}$$

it is easier to convince a person with no preconceived belief than to convince a person to change their mind. It is, in other words, a *relative stubborness* clause. Factoring in the parameters α_p and α_q, this gives us

$$\begin{aligned} \delta_q &\leq \alpha_q \leq 1 \\ \delta_p &\leq \alpha_p \leq 1 \end{aligned} \tag{5}$$

One case of special interested will be that in which one of the two parameters α_p or α_q vanishes. If we assume, for example, that p is truthful information and q a piece of fake news, setting $\alpha_q = 0$ entails that people who believe the fake news can verify it and change their mind, while people who believe the truth will not find any factual support for, and never switch directly to, falsehood. We can call these individuals *limited-information rational believers*: they may believe the false news, but only as long as they had no chance of verifying them: once they check and know the news are false, they switch to the truth.

The situation are symmetric so, for the sake of simplification, we shall always assume that p is the truth, so $\alpha_p > 0$ always, while α_q can be equal to zero. In this case, of course, convincing from p to q is not effective in the sense of (3) (the limited resilience clause does not apply to the direct change from truth to falsehood, which is assumed to be impossible).

Define the *effective infection rates* as

$$\begin{aligned} \tau &= \frac{\beta_p}{\delta_p} \\ \theta &= \frac{\beta_q}{\delta_q} \end{aligned} \tag{6}$$

and the *recovery ratio* as

$$\xi = \frac{\delta_p}{\delta_q}. \tag{7}$$

In all the following, we shall consider situations in which τ and θ are variables, but they change in such a way

that ξ remains constant. The effective infection rate of a meme is the average number of people a believer convinces before ceasing proselytism [7], that is, it is a measure of the penetration power of a meme.

The model is a Markov process with a state-space given by the set of states of all the nodes. The model quickly becomes intractable for large networks, since the state space grows as $\Theta(3^N)$. The problem can be simplified with suitable approximations. In particular, let $s_i(t)$, $p_i(t)$ and $q_i(t)$ are the probabilities that node i be in state S, P, Q (respectively) at time t. For future use, we define the vectors $s = [s_1, \dots, s_N]'$ $p = [p_1, \dots, p_N]'$ and $q = [q_1, \dots, q_N]'$.

In the mean field approximation [27], we can write the evolution equations for p and q as

$$\begin{aligned}\dot{p}_i &= \big[\beta_p s_i + \beta_{qp} q_i\big] \sum_{j=1}^{N} a_{ij} p_j - \beta_{pq} p_i \sum_{j=1}^{N} b_{ij} q_j - \delta_p p_i \\ \dot{q}_i &= \big[\beta_q s_i + \beta_{pq} p_i\big] \sum_{j=1}^{N} b_{ij} q_j - \beta_{qp} q_i \sum_{j=1}^{N} a_{ij} p_j - \delta_q q_i\end{aligned} \tag{8}$$

or, with the definitions in (6) and (7),

$$\begin{aligned}\frac{1}{\delta_p}\dot{p} &= \tau\big[s_i + \alpha_q q_i\big] \sum_{j=1}^{N} a_{ij} p_j - \theta \frac{\alpha_p}{\xi} p_i \sum_{j=1}^{N} b_{ij} q_j - p_i \\ \frac{1}{\delta_q}\dot{q} &= \theta\big[s_i + \alpha_p p_i\big] \sum_{j=1}^{N} b_{ij} q_j - \tau \alpha_q \xi q_i \sum_{j=1}^{N} a_{ij} p_j - q_i\end{aligned} \tag{9}$$

The two equations are symmetric: one can be transformed into the other via the transformation

$$p_i \leftrightarrow q_i \;\; \alpha_p \leftrightarrow \alpha_q \;\; \tau \leftrightarrow \theta \;\; \xi \leftrightarrow \frac{1}{\xi}. \tag{10}$$

This transformation will be useful in the following to extend properties and results from one meme to the other.

3 Types of equilibria

The equilibrium solution for the two equations is given by

$$\begin{aligned}p^* &= \tau\big[(1 - p_i - q_i) + \alpha_q q_i^*\big] \sum_{j=1}^{N} a_{ij} p_j^* - \theta \frac{\alpha_p}{\xi} p_i^* \sum_{j=1}^{N} b_{ij} q_j^* \\ q^* &= \theta\big[(1 - p_i - q_i) + \alpha_p p_i^*\big] \sum_{j=1}^{N} b_{ij} q_j^* - \tau \alpha_q \xi q_i^* \sum_{j=1}^{N} a_{ij} p_j^*,\end{aligned} \tag{11}$$

where we have used $s_i + p_i + q_i = 1$. We are interested in studying the properties of these equilibrium solutions. We consider four classes of equilibria:

- **I** *meme extincion equilibrium*: none of the two memes survives in the long term and they both die out as $t \to \infty$, that is, in term of the stable solution, $p_i^* = q_i^* = 0$;
- **II** p *dominance*: the meme p dominates until, at $t \to \infty$, q disappear. In this case, $q_i^* = 0$ and p_i^* is given by

$$\frac{p_i^*}{1 - p_i^*} = \tau \sum_{j=1}^{N} a_{ij} p_j^*; \tag{12}$$

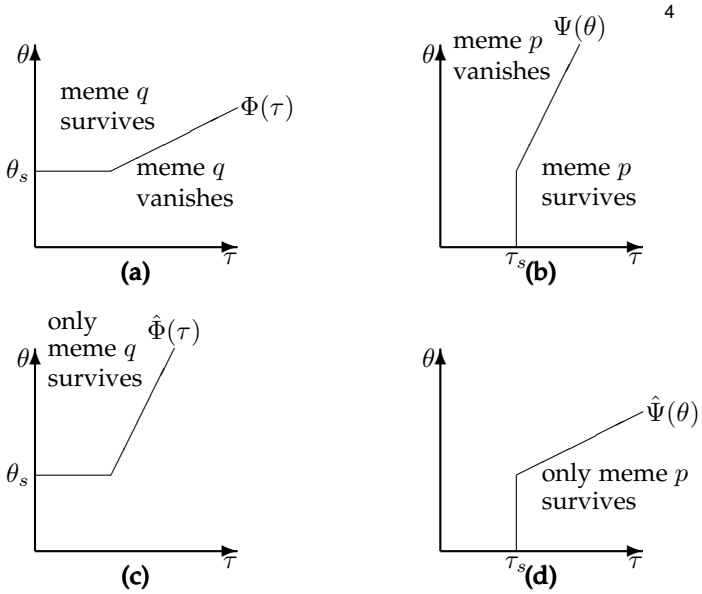

Fig. 2. Qualitative illustration of survival and absolute dominance. In the area $\tau < \tau_s$ and $\theta < \theta_s$ both memes vanish. In **(a)**, meme q survives if its effective infection rate is $\theta > \Phi(\tau)$, and vanishes otherwise. Similarly, in **(b)**, meme p survives if $\tau > \Psi(\theta)$ and vanishes otherwise. In **(c)**, whenever $\theta > \hat{\Phi}(\tau)$, meme q dominates absolutely, that is, meme p vanishes and, similarly in **(d)** if $\tau > \hat{\Psi}(\theta)$, meme p dominates and meme q vanishes. The figure illustrates how the four curves Ψ, $\hat{\Psi}$, Φ, and $\hat{\Phi}$ are not independent, as the region of absolute dominance of a meme corresponds to the region in which the other vanishes.

- **III** q *dominance*: symmetric to the previous one. Now $p_i^* = 0$ and q_i^* is given by

$$\frac{q_i^*}{1 - q_i^*} = \theta \sum_{j=1}^{N} b_{ij} q_j^*; \tag{13}$$

- **IV** *coexistence*: in this case both memes remain active as $t \to \infty$, that is $p_i^* \geq 0$ and $q_i^* \geq 0$

For each value of τ, we define two critical values of θ, which we indicate as $\theta' = \Phi(\tau)$ and $\theta'' = \hat{\Phi}(\tau)$. The first value is the *survival threshold*: given an effective infection rate τ for meme p, if $\theta < \Phi(\tau)$, meme q vanishes. The second is the *absolute dominance* threshold: given a value of τ for p, if $\theta > \hat{\Phi}(\tau)$ q dominates and p vanishes. Similar thresholds are defined for τ: $\tau' = \Psi(\theta)$, $\tau'' = \hat{\Psi}(\theta)$.

In addition to these, there are the *absolute survival thresholds* τ_s and θ_s, defined by $\tau_s = \Psi(\theta_s), \theta_s = \Phi(\tau_s)$ below which a meme vanishes independently of the presence and the behavior of the other. If $\tau < \tau_s$, then p vanishes unconditionally, therefore

$$\tau < \tau_s \implies \Phi(\tau) = \hat{\Phi}(\tau) = \theta_s \tag{14}$$

and, similarly,

$$\theta < \theta_s \implies \Psi(\theta) = \hat{\Psi}(\theta) = \tau_s \tag{15}$$

The values $\Phi(\tau)$, $\hat{\Phi}(\tau)$, $\Psi(\theta)$, and $\hat{\Psi}(\theta)$ are not independent: beyond the absolute survival threshold, q survives if and only if p does not dominate, and vice-versa. That is, given a value $\tau > \tau_s$, the condition $\theta < \Phi(\tau)$ determines at the same time the vanishing of q and the dominance of p, and the same holds for $\tau < \Psi(\theta)$. The situation is depicted schematically in Figure 2. The figure shows that the region of absolute dominance of one meme corresponds

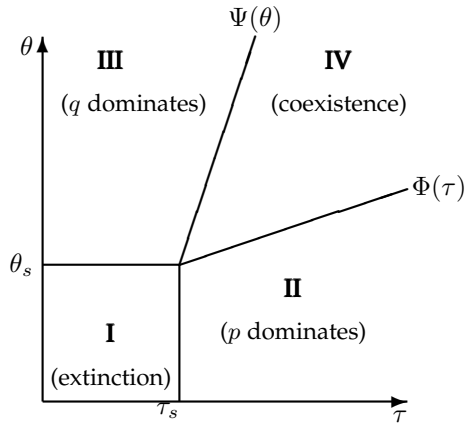

Fig. 3. The four regions describing the possible outcomes of the interaction between the two memes. In region **I** both memes die out, in region **II** meme p dominates and meme q dies out, in region **III** the opposite is true: q dominates and p dies out; finally, in region **IV** there is coexistence: both memes survive. The situation can be described completely once we determine the values θ_s and τ_s and the curves $\Phi(\tau)$ and $\Psi(\theta)$.

to the region beyond the absolute survival threshold where the other vanishes. That is, for $\tau > \tau_s$ and $\theta > \theta_s$, we have

$$\begin{aligned}\hat{\Psi}(\theta) &= \Phi^{-1}(\theta)\\ \hat{\Phi}(\tau) &= \Psi^{-1}(\tau).\end{aligned} \tag{16}$$

In the following, we shall consider only the curves $\Phi(\tau)$ and $\Psi(\theta)$. These considerations also give us a qualitative schema for the relation between the four regions I–IV mentioned above (Figure 3).

3.1 Extinction of both memes

The analysis of region I is quite similar to the analysis carried out in [27]. Region I is the region of stability of the solution $p_i = q_i = 0$. Consider first $q_i = 0$. In this case the solution for p_i is the solution of

$$\dot{p_i} = \tau(1 - p_i)\sum_j a_{ij}p_j - p_i, \tag{17}$$

that is,

$$\dot{p} = \big[\tau\mathrm{diag}(1 - p_i)\mathbf{A} - \mathbf{I}\big]p. \tag{18}$$

The solution $p = 0$ is stable is all the eigenvalues of $[\tau\mathrm{diag}(1 - p_i)\mathbf{A} - \mathbf{I}]|_{p=0}$ are negative[1], that is if $\lambda_1(\tau\mathbf{A} - \mathbf{I}) < 0$, where λ_1 is the largest eigenvalue of the matrix. This leads to

$$\tau_s = \frac{1}{\lambda_{\mathbf{A}}}. \tag{19}$$

Reasoning in the same way with $p = 0$, the equation for q leads to

$$\theta_s = \frac{1}{\lambda_{\mathbf{B}}}. \tag{20}$$

1. Technically, if they have negative real part. However, the matrices involved are symmetric and therefore all their eigenvalues are real.

3.2 Border of regions II and III

Consider region II, in which $p_i \geq 0$, $q_i = 0$. Since $q_i = 0$, the equilibrium solution of p is determined by (12). The border between region II and IV is given by the stability of the solution $q_i = 0$ under the condition that p be given by (12). We write the equation for q in the form $\dot{q} = G(q)\,q$, with, from (9):

$$G_i(q) = \theta\big[s_i + \alpha_p p_i\big]\sum_{j=1}^{N} b_{ij}q_j - \alpha_q\xi\tau q_i\sum_{j=1}^{N} a_{ij}p_j - q_i; \tag{21}$$

writing $s_i = 1 - p_i - q_i$, we have

$$G_i(q) = \theta\big[1-q_i-(1-\alpha_p)p_i\big]\sum_{j=1}^{N} b_{ij}q_j-\alpha_q\xi\tau q_i\sum_{j=1}^{N} a_{ij}p_j-q_i. \tag{22}$$

The stability is given in this case by the eigenvalues of ∇G computed in $q = 0$. To determine $\nabla G_i|_0$ we compute

$$\begin{aligned}\left.\frac{\partial G_i}{\partial q_j}\right|_0 &= \theta\big[1 - (1 - \alpha_p)p_i\big]b_{ij} - \alpha_q\xi\tau\sum_{j=1}^{N} a_{ij}p_j\delta_{ij} - \delta_{ij}\\ &= \theta\big[1 - (1 - \alpha_p)p_i\big]b_{ij} - \alpha_q\xi\frac{p_i}{1 - p_i}\delta_{ij} - \delta_{ij},\end{aligned} \tag{23}$$

from which

$$\nabla G|_0 = \theta\big[\mathbf{I} - (1 - \alpha_p)\mathrm{diag}(p_i)\big]\mathbf{B} - \alpha_q\xi\mathrm{diag}\big(\frac{p_i}{1 - p_i}\big) - \mathbf{I}. \tag{24}$$

The stability condition $\lambda_1(\nabla G) < 0$ leads to the implicit equation for the boundary $\Phi(\tau)$

$$\lambda_1\big[\Phi(\tau)\big(\mathbf{I} - (1 - \alpha_p)\mathrm{diag}(p_i)\big)\mathbf{B} - \alpha_q\xi\mathrm{diag}\big(\frac{p_i}{1 - p_i}\big)\big] = 1. \tag{25}$$

Symmetry and the application of (10) lead to an implicit equation for $\Psi(\theta)$:

$$\lambda_1\big[\Psi(\theta)\big(\mathbf{I} - (1 - \alpha_q)\mathrm{diag}(q_i)\big)\mathbf{A} - \frac{\alpha_p}{\xi}\mathrm{diag}\big(\frac{q_i}{1 - q_i}\big)\big] = 1. \tag{26}$$

4 Guiding example: regular graphs

Equations (25) and (26) cannot in general be solved analytically, and in the following section we shall do a qualitative study for $\tau \sim \frac{1}{\lambda_{\mathbf{A}}}, \theta \sim \frac{1}{\lambda_{\mathbf{B}}}$ as well as for the cases $\tau \to \infty$ and $\theta \to \infty$.

Before we do that, however, in this section, we do a quantitative study of a special case, namely that of *regular graphs*. This example will allow us to do some qualitative considerations of general validity, and will work as a special case on which we shall build the more general considerarions of the following section.

Assume that the two sets of edges A and B are regular, so that in A each node has m_a neighbors, and in B each node has m_b. In terms of the matrices $\mathbf{A}$ and $\mathbf{B}$, this entails that $\sum_j a_{ij} = m_a$ and $\sum_j b_{ij} = m_b$ for all i.

Let $p = \mathfrak{p}\mathbf{1}$, with $\mathfrak{p} > 0$ and $\mathbf{1} = [1, 1, \ldots, 1]'$ and, similarly, $q = \mathfrak{q}\mathbf{1}$. Then

$$\begin{aligned}\mathbf{A}p &= \mathfrak{p}\mathbf{A}\mathbf{1} = \mathfrak{p}m_a\mathbf{1} = m_a p\\ \mathbf{B}q &= \mathfrak{q}\mathbf{B}\mathbf{1} = \mathfrak{q}m_b\mathbf{1} = m_b q,\end{aligned} \tag{27}$$

that is, m_a is an eigenvalue of $\mathbf{A}$ and m_b of $\mathbf{B}$. Since all the elements of p and q are positive, the Perron-Frobenius theorem entails that $m_a = \lambda_{\mathbf{A}}$ and $m_b = \lambda_{\mathbf{B}}$.

For $\tau < \frac{1}{m_a}, \theta < \frac{1}{m_b}$ we are in region I and both memes vanish. Consider now region II. From (12) we have

$$\mathfrak{p} = 1 - \frac{1}{\tau m_a} = 1 - \frac{1}{\tau \lambda_{\mathbf{A}}}, \tag{28}$$

therefore

$$\begin{aligned} p_i &= 1 - \frac{1}{\tau \lambda_{\mathbf{A}}}, \\ \frac{p_i}{1-p_i} &= \tau \lambda_{\mathbf{A}} - 1, \end{aligned} \tag{29}$$

and

$$\begin{aligned} \mathrm{diag}(p_i) &= \big(1 - \frac{1}{\tau \lambda_{\mathbf{A}}}\big)\mathbf{I}, \\ \mathrm{diag}\big(\frac{p_i}{1-p_i}\big) &= (\tau \lambda_{\mathbf{A}} - 1)\mathbf{I}. \end{aligned} \tag{30}$$

With this we rewrite (25) as

$$\lambda_1\big[\Phi(\tau)\frac{1}{\tau\lambda_{\mathbf{A}}}[1+\alpha_p(\tau\lambda_{\mathbf{A}}-1)]\mathbf{B} - \alpha_q\xi(\tau\lambda_{\mathbf{A}}-1)\mathbf{I}\big] = 1, \tag{31}$$

which leads to

$$\Phi(\tau) = \frac{1}{1+\alpha_p(\tau\lambda_{\mathbf{A}}-1)}\Big[\tau\frac{\lambda_{\mathbf{A}}}{\lambda_{\mathbf{B}}}\big[1+\alpha_q\xi(\tau\lambda_{\mathbf{A}}-1)\big]\Big] \tag{32}$$

and, through (10):

$$\Psi(\theta) = \frac{1}{1+\alpha_q(\theta\lambda_{\mathbf{B}}-1)}\Big[\theta\frac{\lambda_{\mathbf{B}}}{\lambda_{\mathbf{A}}}\big[1+\frac{\alpha_p}{\xi}(\theta\lambda_{\mathbf{B}}-1)\big]\Big]. \tag{33}$$

The derivatives of Φ and Ψ at the survival critical point ($\tau = \tau_s$ and $\theta = \theta_s$) determine the existence of a critical region. We have

$$\begin{aligned} \frac{d}{d\tau}\Phi =& \frac{-\alpha_p\lambda_{\mathbf{A}}}{[1+\alpha_p(\tau\lambda_{\mathbf{A}}-1)]^2}\tau\frac{\lambda_{\mathbf{A}}}{\lambda_{\mathbf{B}}}\Big[1+\alpha_q\xi(\tau\lambda_{\mathbf{A}}-1)\Big] \\ &+ \frac{1}{1+\alpha_p(\tau\lambda_{\mathbf{A}}-1)}\frac{\lambda_{\mathbf{A}}}{\lambda_{\mathbf{B}}}\Big[1+2\alpha_1\xi\lambda_{\mathbf{A}}\tau-\alpha_q\xi\Big] \end{aligned} \tag{34}$$

and

$$\left.\frac{d\Phi\tau}{d\tau}\right|_{\tau=1/\lambda_{\mathbf{A}}} = \frac{\lambda_{\mathbf{A}}}{\lambda_{\mathbf{B}}}[\alpha_q\xi - \alpha_p + 1]. \tag{35}$$

Finally, applying (10):

$$\left.\frac{d\Psi\theta}{d\theta}\right|_{\theta=1/\lambda_{\mathbf{B}}} = \frac{\lambda_{\mathbf{B}}}{\lambda_{\mathbf{A}}}[\frac{\alpha_p}{\xi} - \alpha_q + 1]. \tag{36}$$

We use these results to determine the existence of a zone of coexistence (zone IV) in two cases: "weak" memes (memes near the vanishing points, viz., $\tau \sim 1/\lambda(\mathbf{A})$ and $\theta \sim 1/\lambda(\mathbf{B})$) and "aggressive" memes ($\tau \to \infty$ and $\theta \to \infty$).

Consider weak memes first. There is coexistence if

$$\frac{d\Phi}{d\tau}\frac{d\Psi}{d\theta} < 1, \tag{37}$$

that is

$$(\alpha_q\xi - \alpha_p + 1)(\frac{\alpha_p}{\xi} - \alpha_q + 1) < 1, \tag{38}$$

which gives:

$$[\frac{1}{\xi} + (\alpha_q - \frac{\alpha_p}{\xi})][1 - (\alpha_q - \frac{\alpha_p}{\xi})] < \frac{1}{\xi}, \tag{39}$$

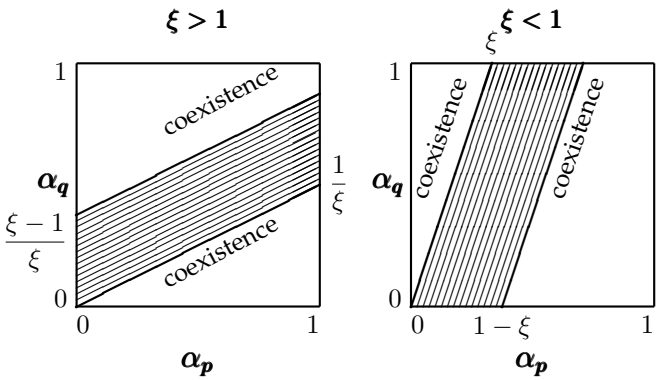

Fig. 4. Regions in the space α_p, α_q that allow the coexistence of two "weak" memes ($\tau \sim 1/\lambda(\mathbf{A})$, $\theta \sim 1/\lambda(\mathbf{B})$) in a regular graph. In the shaded region, no coexistence is possible: one of the two memes will dominate and the other will vanish. The first figure refers to the case $\xi > 1$, viz, $\delta_p > \delta_q$, the second to the case $\xi < 1$.

leading to

$$(\alpha_q - \frac{\alpha_p}{\xi})[\frac{\xi-1}{\xi} - (\alpha_q - \frac{\alpha_p}{\xi})] < 0. \tag{40}$$

If $\xi > 1$, the solutions are

$$\begin{aligned} \alpha_q &< \frac{\alpha_p}{\xi} \\ \alpha_q &> \frac{\alpha_p}{\xi} + \frac{\xi-1}{\xi} \end{aligned} \tag{41}$$

while for $\xi < 1$

$$\begin{aligned} \alpha_q &> \frac{\alpha_p}{\xi} \\ \alpha_q &< \frac{\alpha_p}{\xi} - \frac{1-\xi}{\xi}. \end{aligned} \tag{42}$$

The two coexistence regions are illustrated in Figure 4.

For aggressive memes, if $\tau\lambda_A \gg 1$ and $\theta\lambda_B \gg 1$ we can approximate (32) as

$$\Phi(\tau) \sim \begin{cases} \frac{\lambda_{\mathbf{A}}}{\lambda_{\mathbf{B}}}\tau + \alpha_q\xi\frac{\lambda_{\mathbf{A}}^2}{\lambda_{\mathbf{B}}}\tau^2 & \alpha_p = 0 \\ \frac{1}{\alpha_p\lambda_{\mathbf{B}}} + \frac{\alpha_q}{\alpha_p}\frac{\lambda_{\mathbf{A}}}{\lambda_{\mathbf{B}}}\xi\tau & \alpha_p > 0 \end{cases} \tag{43}$$

and (33) as

$$\Psi(\tau) \sim \begin{cases} \frac{\lambda_{\mathbf{B}}}{\lambda_{\mathbf{A}}}\theta + \frac{\alpha_p}{\xi}\frac{\lambda_{\mathbf{B}}^2}{\lambda_{\mathbf{A}}}\theta^2 & \alpha_q = 0 \\ \frac{1}{\alpha_q\lambda_{\mathbf{A}}} + \frac{\alpha_p}{\alpha_q}\frac{\lambda_{\mathbf{B}}}{\lambda_{\mathbf{A}}}\frac{1}{\xi}\theta & \alpha_q > 0. \end{cases} \tag{44}$$

We have to consider four cases.

$\alpha_p = \alpha_q = 0$

this reduces our model to that in [27]. In this case

$$\begin{aligned} \Phi(\tau) &\sim \frac{\lambda_{\mathbf{A}}}{\lambda_{\mathbf{B}}}\tau \\ \Psi(\theta) &\sim \frac{\lambda_{\mathbf{B}}}{\lambda_{\mathbf{A}}}\theta. \end{aligned} \tag{45}$$

The two lines are parallel, therefore there is a coexistence region only if there was one for weak memes. In particular, we find again the result in [27]: if the two memes spread on the same graph ($\mathbf{A} = \mathbf{B}$) there can be no coexistence.

$\alpha_p = 0$, $\alpha_q > 0$
In this case

$$\begin{aligned}\Phi(\tau) &\sim \frac{\lambda_{\mathbf{A}}}{\lambda_{\mathbf{B}}}\tau + \alpha_q \xi \frac{\lambda_{\mathbf{A}}^2}{\lambda_{\mathbf{B}}}\tau^2 \\ \Psi(\theta) &\sim \frac{1}{\alpha_q \lambda_{\mathbf{A}}}.\end{aligned} \tag{46}$$

and there is always a coexistence region
$\alpha_q = 0$, $\alpha_p > 0$
This case is analogous to the previous one: there is always coexistence.
$\alpha_p > 0$, $\alpha_q > 0$
In this case

$$\begin{aligned}\Phi(\tau) &\sim \frac{1}{\alpha_p \lambda_{\mathbf{B}}} + \frac{\alpha_q}{\alpha_p}\frac{\lambda_{\mathbf{A}}}{\lambda_{\mathbf{B}}}\xi\tau \\ \Psi(\theta) &\sim \frac{1}{\alpha_q \lambda_{\mathbf{A}}} + \frac{\alpha_p}{\alpha_q}\frac{\lambda_{\mathbf{B}}}{\lambda_{\mathbf{A}}}\frac{1}{\xi}\theta.\end{aligned} \tag{47}$$

Here too we have two parallel lines but, since the constant terms are always positive, there is always a coexistence region.

5 The General Case

We now consider the case of a general multi-network, beginning with weak memes, near the critical point. Considering $\Phi(\tau)$, near the critical point we have

$$\Phi(\tau) = \frac{1}{\lambda_{\mathbf{B}}} + \frac{d}{d\tau}\Phi\Big|_{1/\lambda_{\mathbf{A}}} (\tau - \frac{1}{\lambda_{\mathbf{A}}}) + O\left((\tau - \frac{1}{\lambda_{\mathbf{A}}})^2\right). \tag{48}$$

The derivative is computed at the point $\tau = 1/\lambda_{\mathbf{A}}$, $\theta = 1/\lambda_{\mathbf{B}}$ with $p_i = q_i = 0$. From (25) we have

$$\frac{\partial \lambda_1}{\partial \Phi}\frac{d\Phi}{d\tau} + \frac{\partial \lambda_1}{\partial \tau} = 0. \tag{49}$$

The first term is

$$\frac{\partial \lambda}{\partial \Phi} = \lambda_1\big[(\mathbf{I} - (1-\alpha_p)\mathrm{diag}(p_i))\mathbf{B}\big]\big|_{p_i=0} = \lambda_{\mathbf{B}}. \tag{50}$$

In order to compute the secod term, define

$$\begin{aligned}\mathbf{M}_1 &= (\mathbf{I} - (1-\alpha_p)\mathrm{diag}(p_i))\mathbf{B} \\ \mathbf{M}_2 &= \alpha_q \xi \mathrm{diag}\big(\frac{p_i}{1-p_i}\big).\end{aligned} \tag{51}$$

With these definitions we have

$$\frac{\partial \lambda_1}{\partial \tau} = \sum_{i=1}^{N}\frac{\partial \lambda_1}{\partial p_i}\frac{dp_i}{d\tau} = \sum_{i=1}^{N}\mathfrak{b}'\Big[\frac{\partial \mathbf{M}_1}{\partial p_i} - \frac{\partial \mathbf{M}_2}{\partial p_i}\Big]\mathfrak{b}, \tag{52}$$

where $\mathfrak{b}$ is the (normalized) eigenvector associated to

$$\lambda_1[\mathbf{M}_1 - \mathbf{M}_2]\big|_{p_i=0} = \lambda_{\mathbf{B}}. \tag{53}$$

This leads to

$$\begin{aligned}\frac{\partial \mathbf{M}_1}{\partial p_i} &= -\phi(1-\alpha_p)\begin{bmatrix} 0 & \cdots & 0 \\ & \ddots & \\ & 1 & \\ & & \ddots \\ 0 & \cdots & 0 \end{bmatrix}\mathbf{B} \\ &= -\frac{1-\alpha_p}{\lambda_{\mathbf{B}}}\begin{bmatrix} & 0 & \\ & \vdots & \\ b_{i1} & \cdots & b_{in} \\ & \vdots & \\ & 0 & \end{bmatrix},\end{aligned} \tag{54}$$

where, in the second equality, we have considered that we are computing the derivative in $\tau = 1/\lambda_{\mathbf{A}}$ and that $\Phi(1/\lambda_{\mathbf{A}}) = 1/\lambda_{\mathbf{B}}$. With this, and considering that $\mathbf{B}\mathfrak{b} = \lambda_{\mathbf{B}}\mathfrak{b}$, we have

$$\begin{aligned}\frac{\partial \mathbf{M}_1}{\partial p_i}\mathfrak{b} &= -\frac{1-\alpha_p}{\lambda_{\mathbf{B}}}\big[0, \ldots, \sum_k b_{ik}\mathfrak{b}_k, \ldots, 0\big]' \\ &= -(1-\alpha_p)\big[0, \ldots, \mathfrak{b}_i, \ldots, 0\big]'\end{aligned} \tag{55}$$

and

$$\mathfrak{b}'\frac{\partial \mathbf{M}_1}{\partial p_i}\mathfrak{b} = -(1-\alpha_p)\mathfrak{b}_i^2. \tag{56}$$

With similar considerations we obtain

$$\mathfrak{b}'\frac{\partial \mathbf{M}_2}{\partial p_i}\mathfrak{b} = \frac{\xi\alpha_q}{(1-p_i)^2}\mathfrak{b}_i^2\Big|_{p_i=0} = \xi\alpha_q\mathfrak{b}_i^2, \tag{57}$$

leading to

$$\frac{\partial \lambda_1}{\partial p_i} = -[1 - \alpha_p - \xi\alpha_q]\mathfrak{b}_i^2. \tag{58}$$

In order to compute $dp_i/d\tau$, we use (12). From

$$p_i = \tau(1-p_i)\sum_{k=1}^{N} a_{ik}p_k \tag{59}$$

we get

$$\frac{dp_i}{d\tau} = (1-p_i)\sum_{k=1}^{N} a_{ik}p_k - \tau\sum_{k=1}^{N} a_{ik}p_k + \tau(1-p_i)\sum_{k=1}^{N} a_{ik}\frac{dp_k}{d\tau} \tag{60}$$

which, at the critical point, reduces to

$$\frac{dp_i}{d\tau} = \frac{1}{\lambda_{\mathbf{A}}}\sum_{k=1}^{N} a_{ik}\frac{dp_k}{d\tau}. \tag{61}$$

That is, the vector of derivatives is an eigenvector corresponding to $\lambda_{\mathbf{A}}$. If $\mathfrak{a}$ is the normalized eigenvector for that eigenvalue, then there is a κ such that

$$\frac{dp_i}{d\tau} = \kappa\mathfrak{a}_i. \tag{62}$$

This gives us

$$\frac{\partial \lambda_1}{\partial \tau} = -\kappa[1 - \alpha_p + \xi\alpha_q]\sum_{i=1}^{N}\mathfrak{a}_i\mathfrak{b}_i^2 \tag{63}$$

and, from (49) and (50),

$$\frac{d\Phi}{d\tau} = \kappa\frac{1 - \alpha_p + \xi\alpha_q}{\lambda_{\mathbf{B}}}\sum_{i=1}^{N}\mathfrak{a}_i\mathfrak{b}_i^2. \tag{64}$$

We determine κ by considering the equation in the special cases of the regular graph, which we have analyzed in the previous section, and of [27].

Comparing (35) with (64), we have

$$\frac{\lambda_i(\mathbf{A})}{\lambda_i(\mathbf{B})}[1-\alpha_p+\xi\alpha_q]=\kappa\frac{1-\alpha_p+\xi\alpha_q}{\lambda_{\mathbf{B}}}\sum_{i=1}^{N}\mathfrak{a}_i\mathfrak{b}_i^2. \quad (65)$$

In the case of regular graphs, $\mathfrak{a}_i=\mathfrak{b}_i=1/\sqrt{n}$, therefore

$$\lambda_{\mathbf{A}}=\kappa\sum_{i=1}^{N}\mathfrak{a}_i\mathfrak{b}_i^2=\frac{\kappa}{\sqrt{n}}. \quad (66)$$

The result in [27] suggests that we use the equality $1/\sqrt{n}=\sum_i \mathfrak{b}_i^3$, leading to

$$\kappa=\frac{\lambda_{\mathbf{A}}}{\sum_{i=1}^{N}\mathfrak{b}_i^3}. \quad (67)$$

so we obtain

$$\frac{d\Phi}{d\tau}=\frac{\lambda_{\mathbf{A}}}{\lambda_{\mathbf{B}}}[1-\alpha_p+\xi\alpha_q]\frac{\sum_{i=1}^{N}\mathfrak{a}_i\mathfrak{b}_i^2}{\sum_{i=1}^{N}\mathfrak{b}_i^3}. \quad (68)$$

Application of (10) yields

$$\frac{d\Psi}{d\theta}=\frac{\lambda_{\mathbf{B}}}{\lambda_{\mathbf{A}}}[1-\alpha_q+\frac{\alpha_p}{\xi}]\frac{\sum_{i=1}^{N}\mathfrak{b}_i\mathfrak{a}_i^2}{\sum_{i=1}^{N}\mathfrak{a}_i^3}. \quad (69)$$

The condition for the presence of a coexistence zone for weak memes is

$$\begin{aligned}\frac{d\Phi}{d\tau}\frac{d\Psi}{d\theta}&=[1-\alpha_p+\xi\alpha_q][1-\alpha_q+\frac{\alpha_p}{\xi}]\times\\&\frac{\left(\sum_{i=1}^{N}\mathfrak{b}_i\mathfrak{a}_i^2\right)\left(\sum_{i=1}^{N}\mathfrak{a}_i\mathfrak{b}_i^2\right)}{\left(\sum_{i=1}^{N}\mathfrak{a}_i^3\right)\left(\sum_{i=1}^{N}\mathfrak{b}_i^3\right)}\\&<1.\end{aligned} \quad (70)$$

If the two meme spread in the same graph, this condition reduces to (38)

* * *

Consider now the case of aggressive memes ($\tau\to\infty$, $\theta\to\infty$), beginning with $\Phi(\tau)$. For $\tau\to\infty$, we have, from (12), $p_i\to 1$. Write $p_i\sim 1-k_i/\tau$, with k_i to be determined. Plugging this in (12), we have

$$\frac{\tau}{k_i}(1-\frac{k_i}{\tau})=\tau\sum_{k=1}^{N}a_{ij}(1-\frac{k_i}{\tau})\sim\tau\sum_{k=1}^{N}a_{ij}=\tau d_i^A, \quad (71)$$

where d_i^A is the degree of node i in graph A. This leads to $k_i=1/d_i^A$ and

$$p_i\sim 1-\frac{1}{\tau d_i^A}. \quad (72)$$

With this approximation we have

$$\begin{aligned}\mathrm{diag}(p_i)&\sim\mathbf{I}-\frac{1}{\tau}\mathbf{D}_A^{-1},\\\mathrm{diag}(\frac{p_i}{1-p_i})&\sim\tau\mathbf{D}_A\end{aligned} \quad (73)$$

and (25) can be rewritten as

$$\lambda_1\Big[\frac{\Phi(\tau)}{\tau}\mathbf{D}_A^{-1}(\mathbf{I}+\tau\alpha_p\mathbf{D})\mathbf{B}-\alpha_q\tau\xi\mathbf{D}\Big]=1. \quad (74)$$

That is, $\rho(\mathbf{M})=1$, where

$$\mathbf{M}\stackrel{\triangle}{=}\mathbf{M}_1-\mathbf{M}_2=\frac{\Phi(\tau)}{\tau}\mathbf{D}_A^{-1}(\mathbf{I}+\tau\alpha_p\mathbf{D})\mathbf{B}-\alpha_q\tau\xi\mathbf{D} \quad (75)$$

and ρ is the spectral radius. Since $\rho(\mathbf{M})$ is finite and is a norm, we can assume that there is C such that

$$\rho(\mathbf{M})-\rho(\mathbf{M}_2)=C \quad (76)$$

(viz., either both radii are finite or they are both infinite). Noting that $\rho(\mathbf{D})=d_+^A\stackrel{\triangle}{=}\max\{d_i^A\}$, we have

$$\frac{\Phi(\tau)}{\tau}\rho\big(\mathbf{D}_A^{-1}(\mathbf{I}+\tau\alpha_p\mathbf{D}_A)\mathbf{B}\big)-\alpha_q\tau\xi d_+^A=C. \quad (77)$$

With this approximation we have

$\alpha_p=0$

$$\Phi(\tau)\sim\frac{\alpha_q\xi d_+^A}{\rho(\mathbf{D}_A^{-1}\mathbf{B})}\tau^2, \quad (78)$$

$\alpha_p>0$ setting $\mathbf{I}+\tau\alpha_p\mathbf{D}_A\sim\tau\alpha_p\mathbf{D}_A$:

$$\Phi(\tau)\sim\frac{\alpha_q}{\alpha_p}\frac{\xi d_+^A}{\lambda_B}\tau. \quad (79)$$

For $\Psi(\theta)$, we apply the transformation (10) obtaining

$$\lambda_1\Big[\frac{\Psi(\theta)}{\theta}\mathbf{D}_B^{-1}(\mathbf{I}+\theta\alpha_q\mathbf{D}_B)\mathbf{A}-\frac{\alpha_p}{\xi}\theta\mathbf{D}_B\Big]=1, \quad (80)$$

that is, under the same approximation

$$\frac{\Psi(\theta)}{\theta}\rho\big(\mathbf{D}_B^{-1}(\mathbf{I}+\theta\alpha_q\mathbf{D}_B)\mathbf{A}\big)-\frac{\alpha_p d_+^B}{\xi}\theta=C. \quad (81)$$

In this case

$\alpha_p=0$

$$\Psi(\theta)\sim\frac{C}{\alpha_q\lambda_A} \quad (82)$$

$\alpha_p>0$

$$\Psi(\theta)\sim\frac{\alpha_p}{\alpha_q}\frac{d_+^B}{\xi\lambda_A}\theta \quad (83)$$

The same considerations as in section 4 suggest that there is always a coexistence region for aggressive memes (remember that we consider always $\alpha_q>0$).

6 Simulations

We simulate meme diffusion in the case $\alpha_p=0$. This case, in addition to allowing a clearer verification of the theoretical results, is of considerable practical interest. If p is a true meme and q a false one, then people may directly change opinion from q to p by checking a reliable source, while no reliable source will allow to change from p to q. We are, in other words, assuming rational readers with limited information who may be misled into believing a falsehood but are willing to change their mind upon verification of the source.

The qualitative behavior predicted for Φ and Ψ is shown in Figure 5; $\Phi(\tau)$ shows a quadratic behavior for large τ, while $\Psi(\theta)$ tends to a limit $1/(\alpha_q\lambda_A)$. In the following, we compare the predicted behavior with simulation data for three values of α_q. The two memes spread on the same graph, a scale-free graph generated using the algorithm in

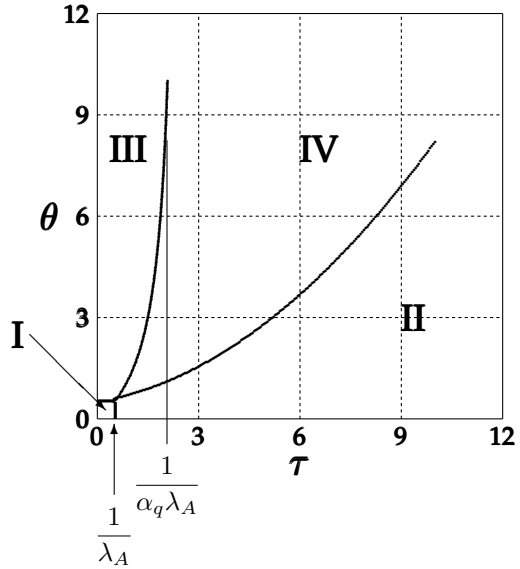

Fig. 5. Qualitative behavior of the coexistence thresholds Φ and Ψ for the case $\alpha_p = 0$ (rational verification: see text). The square at the bottom-left of the figure is the region of non-diffusion: both memes will vanish. The curve Ψ tends to a limit equal to $1/(\alpha_q \lambda_A)$ for $\theta \to \infty$, while $\Phi(\tau)$ goes to infinity like $O(\tau^2)$. The region labels (I–IV) correspond to the regions defined in Section 3.

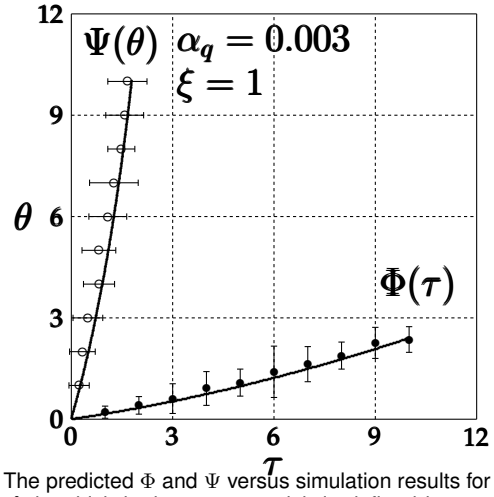

Fig. 6. The predicted Φ and Ψ versus simulation results for $\alpha_q = 0.003$. Region **I**, in which both memes vanish is defined by $\tau, \theta < 1/\lambda_A \approx 0.05$ and is not visible in the diagram. The simulation data are obtained from 20 simulations on the same graph; the figure shows average and standard deviation.

[17], with $N = 5000$ nodes. The graph exhibits a power-law distribution of the type $P[d_i = k] = k^{-\gamma}$. With the parameters used, $\gamma = 2.75$, and the average number of neighbors per node is $\bar{d} = 7.8$, while $\lambda_A = 19.95$. Note that we limit $\alpha_q < 0.05$ because with high values of α_q the simulation becomes unstable for high τ due to the finite number of nodes and of time steps, giving virtually always a dominance of p and making it hard to estimate $\Phi(\tau)$. The values of τ and θ were obtained by manipulating β_p, β_q, δ_p, and δ_q in such as way that $\delta_p = \delta_q$ always, so that $\xi = 1$. The predicted behavior is approximated using the equations (32) and (33) valid for regular graphs, which, in this case, become

$$\begin{aligned} \Phi(\tau) &= \tau\big(1 + \alpha_q \xi(\tau\lambda_A - 1)\big) \\ \Psi(\theta) &= \frac{\theta}{1 + \frac{\alpha_q}{\xi}(\theta\lambda_A - 1)}. \end{aligned} \tag{84}$$

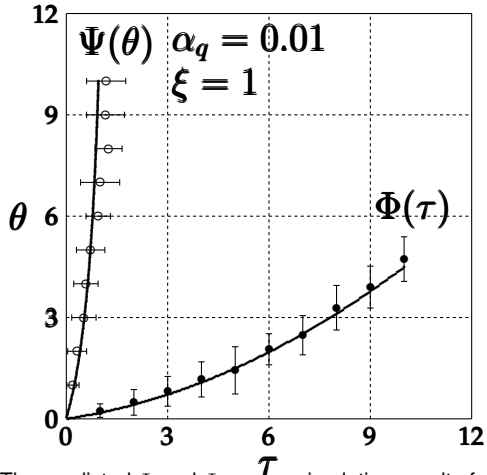

Fig. 7. The predicted Φ and Ψ versus simulation results for $\alpha_q = 0.01$. Region **I**, in which both memes vanish is defined by $\tau, \theta < 1/\lambda_A \approx 0.05$ and is not visible in the diageam. The simulation data are obtained from 20 simulations on the same graph; the figure shows average and standard deviation.

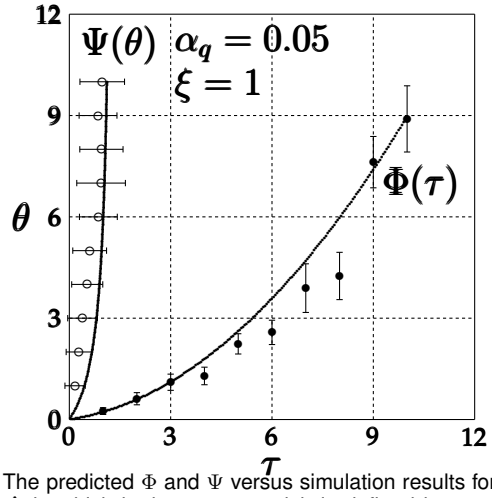

Fig. 8. The predicted Φ and Ψ versus simulation results for $\alpha_q = 0.05$. Region **I**, in which both memes vanish is defined by $\tau, \theta < 1/\lambda_A \approx 0.05$ and is not visible in the diageam. The simulation data are obtained from 20 simulations on the same graph; the figure shows average and standard deviation.

These curves predict quite well the simulated results, well within the standard deviation, for low α_q (Figures 6 and 7), but the predicted behavior is quite off for higher α_q and intermediate values of τ (Figure 8). In this case, the effects of the topology of the network are more evident, and the regular graph approximation is no longer valid.

7 Conclusions

We have extended the model of two-virus spreading to model the possibility of direct change of opinion in meme spread (the possibility of moving from one opinion to another without going through an agnostic state). In particular, we have studied the characteristics of the probability of holding either opinion in the equilibrium when $t \to \infty$.

The possibility of opinion change creates a richer interaction between the two opinions, depending on the three parameters α_p, α_q, ξ. One noteworthy conclusion of our model is that the possibility of direct change allows the coexistence of two opposing memes in the same network, something that in the case of two viruses was ruled out.

REFERENCES

[1] Yong-Yeol Ahn, Hawoong Jeong, Naoki Masuda, and Jae Dong Noh. Epidemic dynamics of two species of interacting particles on scale-free networks. *Physical Review E*, 74(6):066113, 2006.

[2] Sinan Aral and Dylan Walker. Creating social contagion through viral product design: A randomized trial of peer influence in networks. *Management science*, 57(9):1623–39, 2011.

[3] Albert-László Barabási and Réka Albert. Emergence of scaling in random networks. *science*, 286(5439):509–512, 1999.

[4] E. Ben-Naim, P. L. Krapivski, R. Vasquez, and S. Redner. Utility and discord in opinion dynamics. *Physica A*, 330:99–106, 2003.

[5] Béla Bollobás. Random graphs. In *Modern graph theory*, pages 215–52. Springer, 1998.

[6] Claudio Castellano, Santo Fortunato, and Vittorio Loreto. Statistical physics of social dynamics. *Reviews of Modern Physics*, 81:591–646, April–June 2009.

[7] E Cator, R Van de Bovenkamp, and P Van Mieghem. Susceptible-infected-susceptible epidemics on networks with general infection and cure times. *Physical Review E*, 87(6):062816, 2013.

[8] C. Cercignani, R. Illner, and M. Pulvurienti. *The mathematical theory of dilute gases*. Springer Series in Applied Mathematical Sciences. Springer-Verlag, 1994.

[9] Meeyoung Cha, Fabrício Benevenuto, Hamed Haddadi, and Krishna Gummadi. The world of connections and information flow in twitter. *IEEE Transactions on Systems, Man, and Cybernetics-Part A: Systems and Humans*, 42(4):991–8, 2012.

[10] Sebastian Funk and Vincent AA Jansen. Interacting epidemics on overlay networks. *Physical Review E*, 81(3):036118, 2010.

[11] Ayalvadi Ganesh, Laurent Massoulié, and Don Towsley. The effect of network topology on the spread of epidemics. In *Proceedings IEEE 24th Annual Joint Conference of the IEEE Computer and Communications Societies.*, volume 2, pages 1455–66. IEEE, 2005.

[12] Clara Granell, Sergio Gómez, and Alex Arenas. Competing spreading processes on multiplex networks: awareness and epidemics. *Physical review E*, 90(1):012808, 2014.

[13] Christopher Griffin and Richard Brooks. A note on the spread of worms in scale-free networks. *IEEE Transactions on Systems, Man, and Cybernetics, Part B (Cybernetics)*, 36(1):198–202, 2006.

[14] Chunxiao Jiang, Yan Chen, and KJ Ray Liu. Evolutionary dynamics of information diffusion over social networks. *IEEE Transactions on Signal Processing*, 62(17):4573–86, 2014.

[15] Brian Karrer and Mark EJ Newman. Competing epidemics on complex networks. *Physical Review E*, 84(3):036106, 2011.

[16] Mehdi Lallouache, Aninda S. Chakrabarti, Anirban Chakraborti, and Bikas K. Chakrabarti. Opinion formation in the kinetic exchange model: Spontaneous symmetry breaking transition. *Physical Review E - Statistical, Nonlinear and Soft Matter Physics*, 82(5), 2010. arXiv:1007.1790v3 [phycics.soc-ph].

[17] Jure Leskovec, Lars Backstrom, Ravi Kumar, and Andrew Tomkins. Microscopic evolution of social networks. In *Proceedings of the 14th ACM SIGKDD International Conference on Knowledge Discovery and Data Mining*, pages 462–70. ACM, 2008.

[18] Yanbing Mao, Sadegh Bolouki, and Emrah Akyol. Spread of information with confirmation bias in cyber-social networks. *IEEE Transactions on Network Science and Engineering*, 7(2):688–700, 2010.

[19] Alessandro Di Mare and Vito Latora. Opinion formation models based on game theory. *International Journal of Modern Physics C*, 18(9), 2006.

[20] Seth A Myers and Jure Leskovec. Clash of the contagions: Cooperation and competition in information diffusion. In *2012 IEEE 12th international conference on data mining*, pages 539–48. IEEE, 2012.

[21] John Nash. Non-cooperative games. *Annals of Mathematics*, 84(2):286–95, 1951.

[22] Mark EJ Newman and Carrie R Ferrario. Interacting epidemics and coinfection on contact networks. *PloS one*, 8(8):e71321, 2013.

[23] M.E.J. Newman. Threshold effects for two pathogens spreading on a network. *Physical Review Letters*, 95(108701), 2005.

[24] George Orwell. *Nineteen Eighty-Four*. Penguin Classics, 1949.

[25] Chiara Poletto, Sandro Meloni, Vittoria Colizza, Yamir Moreno, and Alessandro Vespignani. Host mobility drives pathogen competition in spatially structured populations. *PLoS Computational Biology*, 9(8):e1003169, 2013.

[26] B Aditya Prakash, Alex Beutel, Roni Rosenfeld, and Christos Faloutsos. Winner takes all: competing viruses or ideas on fair-play networks. In *Proceedings of the 21st international conference on World Wide Web*, pages 1037–46, 2012.

[27] Farayad Darabi Sahneh and Caterina Scoglio. Competitive epidemic spreading over arbitrary multilayer networks. *Physical Review E*, 89(062817), 2014.

[28] Faryad Darabi Sahneh, Caterina Scoglio, and Piet Van Mieghem. Generalized epidemic mean-field model for spreading processes over multilayer complex networks. *IEEE/ACM Transactions on Networking*, 21(5):1609–20, 2013.

[29] Simone Santini. Opinion formation in a locally interacting community with recommender. *arXiv*, 1706.04217, 2017.

[30] Sourya Shrestha, Aaron A King, and Pejman Rohani. Statistical inference for multi-pathogen systems. *PLoS Computational Biology*, 7(8):e1002135, 2011.

[31] Katarina Sznadj-Weron and Jozef Sznadj. Opinion evolution in closed community. *International Journal of Modern Physics C*, 11(6):1157–65, 2000.

[32] Marcella Tambuscio, Giancarlo Ruffo, Alessandro Flammini, and Filippo Menczer. Fact-checking effect on viral hoaxes: A model of misinformation spread in social networks. In *Proceedings of WWW 2015, International World Wide Web Conference*, pages 977–82. ACM, 2015.

[33] Giuseppe Toscani. Kinetic models of opinion formation. *Communications in Mathematical Sciences*, 4(3):481–96, 2006.

[34] Piet Van Mieghem, Jasmina Omic, and Robert Kooij. Virus spread in networks. *IEEE/ACM Transactions On Networking*, 17(1):1–14, 2008.

[35] Yubo Wang, Gaoxi Xiao, and Jian Liu. Dynamics of competing ideas in complex social systems. *New Journal of Physics*, 14(1):013015, 2012.

[36] Xuetao Wei, Nicholas Valler, B Aditya Prakash, Iulian Neamtiu, Michalis Faloutsos, and Christos Faloutsos. Competing memes propagation on networks: a case study of composite networks. *ACM SIGCOMM Computer Communication Review*, 42(5):5–12, 2012.

[37] Xuetao Wei, Nicholas C Valler, B Aditya Prakash, Iulian Neamtiu, Michalis Faloutsos, and Christos Faloutsos. Competing memes propagation on networks: A network science perspective. *IEEE Journal on Selected Areas in Communications*, 31(6):1049–60, 2013.

[38] Lilian Weng, Alessandro Flammini, Alessandro Vespignani, and Fillipo Menczer. Competition among memes in a world with limited attention. *Scientific reports*, 2(1):1–9, 2012.

[39] Qingchu Wu, Michael Small, and Huaxiang Liu. Superinfection behaviors on scale-free networks with competing strains. *Journal of nonlinear science*, 23(1):113–27, 2013.

[40] Yong Zhuang and Osman Yağan. Information propagation in clustered multilayer networks. *IEEE Transactions on Network Science and Engineering*, 3(4):211–24, 2016.